APPLICATION NOTE #APT-36

Advancing Oxide Semiconductors with APT

Quantifying oxygen vacancies in oxide superlattices

The concentration and distribution of oxygen defects can be crucial for the physical properties of complex oxides. Oxygen vacancies, for example, can act as donors and give rise to n-type semiconducting behavior. Furthermore, oxygen defects can impact the magnetic response and lead to fundamentally new functionalities. While the importance of oxygen defects is well known and related effects have been studied in a wide range of materials, their experimental observation remains difficult and quantitative investigations at the atomic level are still a major challenge. In this regard, atom probe tomography (APT) is a promising tool as it allows for quantifying the 3D chemical composition of a material with nanoscale spatial resolution,[1] including light elements such as oxygen.

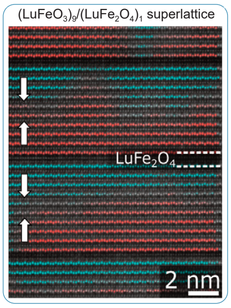

Figure 1:
TEM image of the superlattice structure studied. Red/blue color indicates up/down polarization direction, and the dark lines are the $LuFe_2O_4$ monolayers.
Adapted from ref [2].

As now demonstrated by Hunnestad et al.[2] , APT can provide accurate quantitative information about the 3D distribution of oxygen vacancies within oxide heterostructures. The model system which the team investigated consists of ferroelectric $LuFeO_3$ layers, separated by monolayers of ferrimagnetic $LuFe_2O_4$ as presented in Figure 1. The high-resolution transmission electron microscopy data shows the structure of the superlattice, and the corresponding APT reconstruction is given in Figure 2. The APT data displays both the superlattice and the substrate, visualized by Fe and ZrO ions, respectively. The individual monolayers of $LuFe_2O_4$ are readily visible as darker lines as the $LuFe_2O_4$ phase is nominally enriched in Fe compared to $LuFeO_3$.

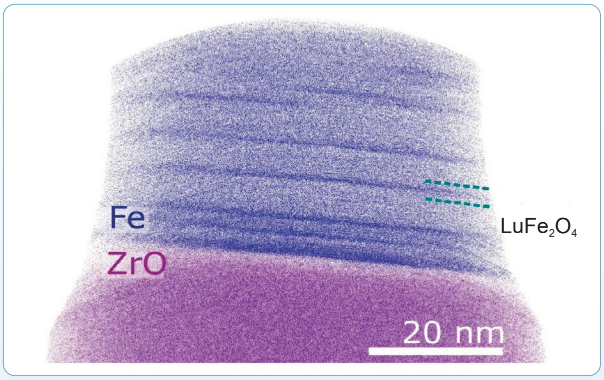

Figure 2:
APT reconstruction of the superlattice. The thin film is visible by the Fe ion distribution, whereas the substrate is shown by the ZrO ions. The dark stripes within the thin film indicate the $LuFe_2O_4$ monolayers.
Adapted from ref [2].

Most interestingly, by extracting the chemical composition in the direction perpendicular to the $LuFe_2O_4$ planes, the team succeeded in resolving local variations in oxygen concentration, as shown in Figure 3. At the $LuFe_2O_4$ monolayers, a strong increase in Fe was measured (dotted line) along with a corresponding decrease in Lu, as expected from the material's composition. In addition, however, it was observed that the O concentration is significantly reduced compared to stoichiometric $LuFe_2O_4$. In comparison to the calculated concentration profile for a defect-free superlattice, the measured O concentration was found to be much lower, revealing an accumulation of oxygen vacancies with a density of (7.8 ±1.8) 10^{13} cm^{-2}. The findings provide new insight into the defect-property relation in complex oxides and demonstrate how oxygen defects correlate with and can promote functional electric and magnetic responses.

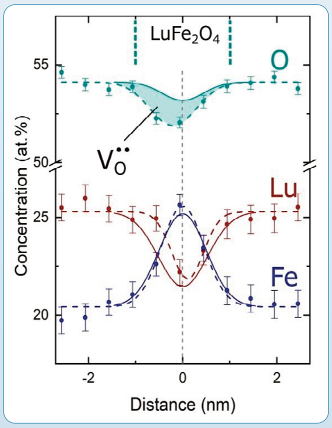

Figure 3:
Profile of the chemical composition across one $LuFe_2O_4$ monolayer. The measured concentration (dotted line) can be seen to deviate from the defect-free concentration (solid line), indicating a presence of oxygen vacancies.
Adapted from ref [2].

The work reveals an innovative application opportunity for APT, enabling quantitative measurements of otherwise hard-to-detect oxygen vacancies, complementing high-resolution structural measurements. The results are of interest for a wide range of systems and make previously hidden oxygen defects in thin films, heterostructures, and superlattices more accessible.

[1] *Hunnestad, K. A. et al. Atomic-scale 3D imaging of individual dopant atoms in an oxide semiconductor. Nat. Commun. 13, 4783 (2022).*
[2] *Hunnestad, K. A. et al. 3D oxygen vacancy distribution and defect-property relations in an oxide heterostructure. Nat. Commun. 15, 1–6 (2024).*

Three Steps to 3D Nanoscale Analysis

An Introduction to Atom Probe Tomography

Step 1: Specimen Preparation

An atom probe specimen usually has a nanoscale region of interest (ROI) requiring both 3D compositional imaging and analysis. The sample is formed into a needle shape containing the ROI. Common APT specimen preparation methods using electropolishing or a Focused Ion Beam system (FIB) are very similar to TEM methods except instead of forming a thin sheet, a needle shaped sample is desired. At the right, standard FIB liftout and mounting of a specimen (figures 1 through 3) and then sharpening the sample with the ROI left at the very apex (4 and 5). In 6, a wire geometry sample is being electropolished.

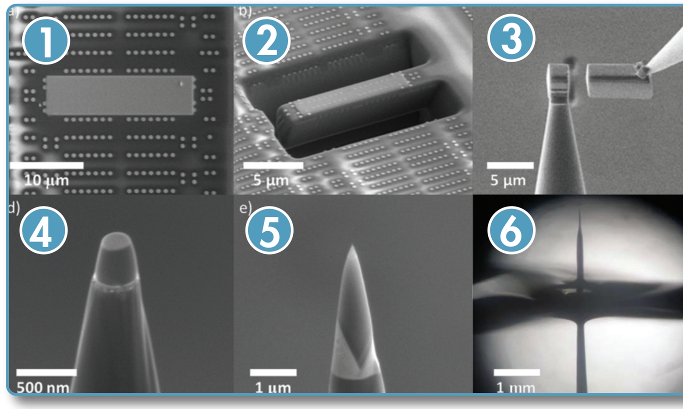

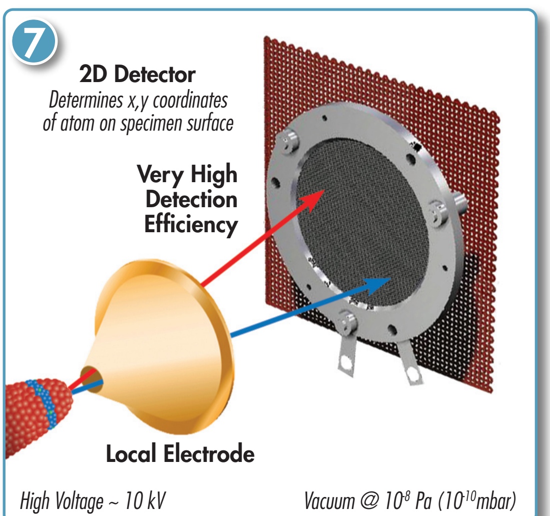

Step 2: Data Collection

An atom probe produces images by field evaporating atoms from a needle-shaped specimen and projecting the resultant ions onto a detector 7.

A high magnification results from the ~ 80nm tip being projected onto an 80mm detector resulting in a magnification of approximately 10^6.

An atom probe identifies atoms by their mass-to-charge-state ratio *(m/n)* using time-of-flight mass spectrometry. Charge state, *n*, is typically 1 to 3.

The specimen is held at approximately 50K to reduce surface diffusion during the experiment. The high electric field results in 100% ionization and the high speed detector is capable of measuring up to 80% of the collected ions, independent of ion mass.

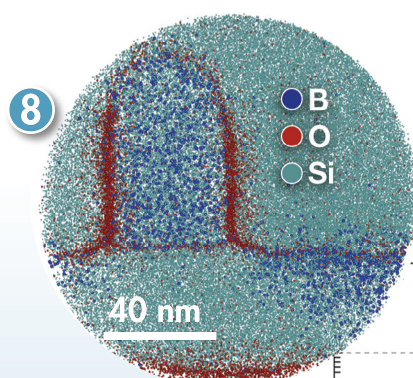

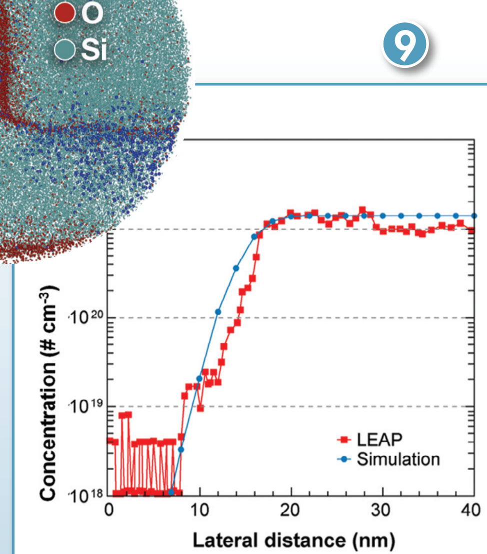

Step 3: Data Visualization and Analysis

Examples of data output are illustrated by a slice of a 3D atom map of a transistor† 8, and a dopant composition profile‡ 9. The image shows the positions of individual atoms (oxygen is red and boron is blue) in the transistor with subnanometer resolution. From the reconstructed data set many types of useful analyses are possible. These include 3D visualization, 2D atom mapping 8, 1D depth profiling and line scanning 9, as well as mass spectra and compositional analysis from user-selected volumes.

† *Lauhon, L. J. et al, MRS Bulletin "Atom Probe Tomography of Semiconductor Materials and Device Structures" 34(10) (2009) 738.*

‡ *Moore, J. S.; Jones, K. S.; Kennel, H.; Corcoran, S., Ultramicroscopy "3-D Analysis of Semiconductor Dopant Distributions in a Patterned Structure using LEAP" (2008), 108, 536–539.*